# Beamline upgrade from PGM (SX700-type) to varied-line-space PGM at CAMD

Masaki Ono, John D. Scott, Eizi Morikawa

*The J. Bennett Johnston, Sr., Center for Advanced Microstructures and Devices (CAMD), Louisiana State University, 6980 Jefferson Highway, Baton Rouge, Louisiana 70806*

**Abstract.** A varied-line-space plane-grating monochromator for the energy range of 200 – 1,200 eV is described as an upgrade of the CAMD plane-grating monochromator. Ray-tracing calculations indicate performance improvements in both resolving power and throughput. An increase in resolving power from ca. 3,000 to the range (from low to high energy) 28,000 – 8,000 throughput increase of 50 – 400% are expected. In contrast to the large enhancement of performance, the proposed modification is relatively inexpensive because of extensive utilization of the current beamline components.

## INTRODUCTION

The CAMD plane grating monochromator (PGM) beamline [1] was commissioned in 1992 as one of the first beamlines at the facility. This PGM was designed as a versatile soft x-ray monochromator that delivers monochromatic photons in the relatively wide energy range of 30 – 1,200 eV with the moderate resolving power of 3,000. By employing an entrance slit, the PGM is capable of operation in either high-resolution or high-throughput mode. After serving for a decade, the PGM's performance no longer meets demands for critical modern research. Furthermore, other soft-x-ray/vuv beamlines (operated below 200 eV) have become operational at CAMD. These factors lead a strong demand for a high performance beamline working over the 200 – 1,200 eV energy range. Our approach is to modify the current PGM beamline instead of constructing a completely new beamline. The proposed modification, namely transforming the PGM to a varied-line-space-plane-grating monochromator (VLSPGM), provides substantial improvements in performance with a relatively small budget.

## CAMD-PGM BEAMLINE

The CAMD-PGM was built based on the SX700 monochromator design developed by H. Petersen [2]. Unlike the original SX700, the CAMD-PGM is equipped with an entrance slit and a spherical focusing mirror (see Fig. 1). Synchrotron radiation from the bending magnet (8 mrad horizontal) is focused vertically onto the entrance slit, and collimated in the horizontal direction, by a pair of (sagittal and meridial-focusing) cylindrical mirrors. Wavelength scan requires rotating a plane-grating in conjunction with translation and rotation of a plane premirror. However, the translation/rotation motion of the premirror is mechanically coupled in the CAMD-PGM, two motion controls, namely the grating rotation and the premirror rotation/translation, are needed for the wavelength scan. The virtual monochromatic source created behind the plane grating at a fixed location (in the fixed-focus operation mode) is focused onto the exit slit by a spherical mirror instead of an ellipsoidal mirror employed in the original SX700 design. Coma aberration introduced by the spherical mirror is minimized by extending the exit arm length of the mirror. The output beam passed through the exit slit is then focused onto a sample position by a toroidal refocusing mirror. The total length of the beamline is approximately 22 meters.

## OPTICAL DESIGN OF VLS-PGM

The advantage of the VLS-PGM (a Hettrick-type) design [3] over the SX700-type is that it can be constructed with fewer optical elements and operated with a simple wavelength scan mechanism. Since only a spherical mirror and a plane grating (VLS) are required, this two-optics design, in principle, provides better throughput efficiency over the three-optics SX700 designs. The VLS-PGM design can be easily adapted from the current CAMD-PGM monochromator mechanism: replacement of the planar premirror with a new spherical mirror, replacement of the plane gratings with new VLS plane gratings, and removal

CP705, *Synchrotron Radiation Instrumentation: Eighth International Conference*, edited by T. Warwick et al.

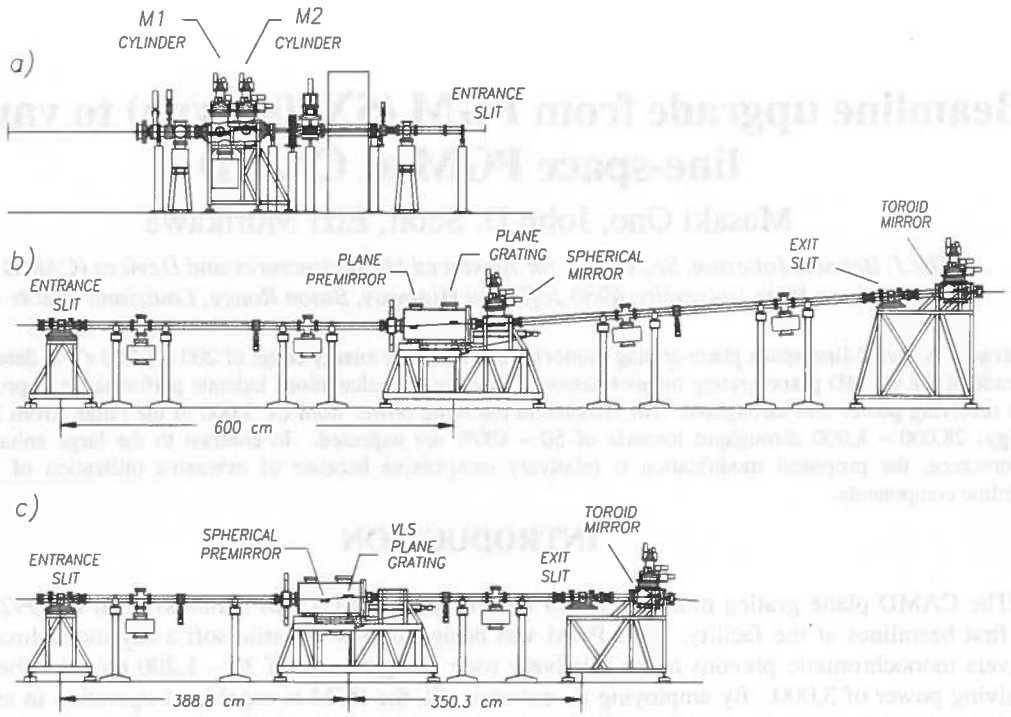


**FIGURE 1.** The CAMD-PGM beamline (a and b) and proposed VLSPGM (a and c).

of the spherical focusing mirror are the only modifications required (see Fig. 1c). The beamline front-end section (M1 and M2 cylindrical mirrors) remain unchanged for the transformation. The support structure for the exit slit and the toroid refocusing mirror requires slight modification. Thus, the transformation to the VLS-PGM design is inexpensive and, more importantly, it promises relatively short commissioning time.

In the VLS grating theory [4, 5], the line space $d$ is a function of the position $w$ in the dispersive (meridian) direction. The function can be expanded as a power series of $w$, namely,

$$d(w) = d_0(1 + b_2 w + b_3 w^2 + b_4 w^3 + \cdots) \tag{1}$$

where $d_0$ is the line space at the center of the grating and $b_2$, $b_3$, and $b_4$ are the space-variation parameters. Diffraction and aberrations caused by the grating are formulated using the light-path function $F(w, l)$,

$$F = F_{00} + wF_{10} + \tfrac{1}{2}w^2F_{20} + \tfrac{1}{2}l^2F_{02} + \tfrac{1}{2}w^3F_{30} + \tfrac{1}{8}w^4F_{40} + \cdots \tag{2}$$

where $l$ is the position in the non-dispersive (sagittal) direction. The coefficients $F_{20}$, $F_{02}$, $F_{30}$ and $F_{40}$ are related to the defocus, the astigmatism, the coma, and the spherical aberration, respectively, and $F_{10}$ corresponds to the diffraction condition. From Eqs. (1) and (2), the following expressions are derived for a plane grating.

$$F_{20} = \left(\frac{\cos^2\alpha}{r_1} + \frac{\cos^2\beta}{r_2}\right) - b_2\frac{m\lambda}{d_0} \tag{3}$$

$$F_{30} = \left( \frac{\sin\alpha \cos^2\alpha}{r_1^2} + \frac{\sin\beta \cos^2\beta}{r_2^2} \right) + \tfrac{2}{3}\left(b_2^2 - b_3\right)\frac{m\lambda}{d_0} \tag{4}$$

$$F_{40} = \left( \frac{\cos^2\alpha\left(4\sin^2\alpha - \cos^2\alpha\right)}{r_1^3} + \frac{\cos^2\beta\left(4\sin^2\beta - \cos^2\beta\right)}{r_2^3} \right) - 2\left(b_2^3 - 2b_2 b_3 + b_4\right)\frac{m\lambda}{d_0} \tag{5}$$

where $m$ is the diffraction order, $\alpha$ is the incidence angle, $\beta$ is the diffraction angle, $r_1$ is the objective distance, and $r_2$ is the image distance. Optimization of the space-variation parameters is made by first determining $b_2$ and $r_2$ by imposing that the defocus, $F_{20}$, vanish at two energies, $E_1$ and $E_2$, then calculating $b_3$ and $b_4$ at the energy $E_2$ with the relation, $F_{30} = F_{40} = 0$. The following values, $\alpha+\beta$ = 174.8°, $r_1$ = -3500 mm, $E_1$ = 500 eV, $E_2$ = 1000 eV, $m$ = 1, $d_0$ = 1.0 x $10^{-3}$ mm (for 400 – 1,200 eV), and $d_0$ = 2.0 x $10^{-3}$ mm (for 200 – 600 eV), provide the VLS parameters: $b_2$ =5.70 x $10^{-4}$ $mm^{-1}$, $b_3$ = 8.15 x $10^{-8}$ $mm^{-2}$, $b_4$ = -4.56 x $10^{-17}$ $mm^{-3}$, $r_2$ = 3502.9 mm. Parameters of the spherical mirror location before the VLS-grating are determined to provide a coma-free entrance slit image at the virtual-image point located behind the VLS-plane grating ($r_1$ = -3500 mm). Table 1 summarizes optical parameters of all VLS-PGM components including the spherical mirror.

**TABLE 1.** Optical parameters of the VLS-PGM beamline.

| | Figure | Radius (cm) | Incidence angle (°) | Distance from source (cm) |
|---|---|---|---|---|
| M1 | Cylindrical | 19.3 | 88.0 | 320 |
| M2 | Cylindrical | 10312 | 88.0 | 360 |
| Entrance slit | | | | 720 |
| M3 (new) | Spherical 8494 | | 87.4 | 1105.3 |
| G (new) | VLS-Plane | | | 1140.6 |
| Exit slit | | | | 1490.9 |
| M4 | Toroid | 4000/5.23 | 88.0 | 1590.9 |
| Sample | | | | 1665.9 |

## CAMD-PGM *vs.* VLS-PGM

Improved performance of the proposed VLS-PGM beamline over the existing PGM beamline was evaluated by SHADOW ray-tracing calculations [6] of the two optical designs. Theoretical resolving power estimated for the VLS-PGM configuration is 28,000 – 8,000 over the range from 200 – 1,200 eV; this is substantial improvement over ca. 3,000 of the current CAMD-PGM. This high-resolution capability is further recognized from the exit slit image given in Fig. 2 where the VLS-PGM is ray-traced with a simulated source consisting of three photon energies.

Throughput from the VLS-PGM is also improved significantly; 50-400% enhancement in flux over that of the CAMD-PGM is expected (see Fig. 3). This is mainly due to the fact that the VLS-PGM configuration consists of one optical component fewer than the CAMD-PGM. At the soft x-ray high-energy region, radiation-intensity attenuation due to reflection is large even at small grazing angle.

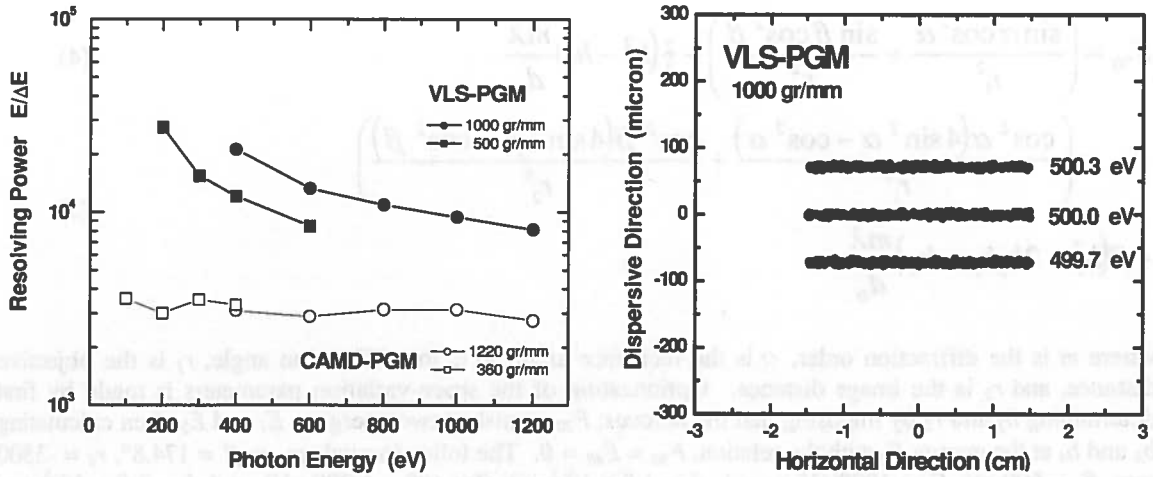


**FIGURE 2.** Resolving power comparison between the VLS-PGM and CAMD-PGM. In the ray-tracing calculations, a rectangular shaped source with 30 mm in horizontal and 10 μm in vertical direction was used. The source angular divergences were set to be zero mrad in horizontal and 2 mrad in vertical direction. All optical components were assumed to have perfect surface figure. Ray-tracing image at the exit slit of the VLS-PGM (right side figure).

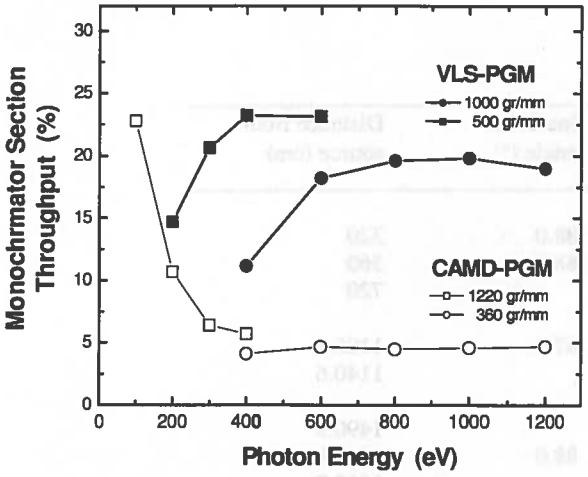


**FIGURE 3.** Throughput comparison between the VLS-PGM and CAMD-PGM. The source described in Fig. 2 was used for ray-tracing the monochromator section. Reflectivity of gold (for the spherical mirror and the plane grating) is included, however, grating efficiency is excluded in the calculations.

## SUMMARY

The ray-tracing calculations confirm that beamline upgrade to the VLS-PGM configuration from the aged PGM beamline provides improved performance in resolving power as well as throughput flux. Since most of beamline components are utilized with little mechanical modifications, the upgrade is relatively inexpensive and requires short commissioning time. This upgrade is a good example of evolution from an existing aged beamline to the next generation.

## REFERENCES

1. Morikawa, E., Scott, J. D., Poliakoff, E. D., Stockbauer, R. L., and Saile, V., Rev. Sci. Instrum., 63, 1300-1304 (1992).
2. Petersen, H., Opt. Commun. 40, 402-406 (1982).
3. Hettrick, M. C., Appl. Opt., 29, 4531-4535 (1990).
4. Koike, M., Beguiristain, R., Underwood, J. H., and Namioka, T., Nucl. Instr. and Meth. A347, 273-277 (1994).
5. Yan, Y., and Yagishita, A., KEK Report 95-9, 1995.
6. Lai, B., Chapman, K., and Cerrina, F., Nucl. Instr. and Meth. A 266, 544-549 (1988).